

Dense gas clouds and the Unidentified EGRET sources

Mark Walker^{1,2}, Masaki Mori³ and Michiko Ohishi³

1. *School of Physics, University of Sydney, NSW 2006, Australia*

2. *Australia Telescope National Facility, CSIRO*

3. *Institute of Cosmic-Ray Research, University of Tokyo, Kashiwa, Chiba 277-8582, Japan*

ABSTRACT

Cold, dense gas clouds have been proposed as a major component of the Galactic dark matter; such clouds can be revealed by the gamma-ray emission which arises from cosmic-rays interacting with the gas. If this dark matter component is clustered then highly luminous GeV sources result, preferentially at low to mid Galactic latitudes where they lie within the cosmic-ray disk. The predicted emission for such clusters is steady, continuum emission with peak power emerging at several hundred MeV. These sources would not have obvious counterparts at other wavelengths and are thus of interest in connection with the UnIDentified (UID) EGRET sources. Here we present a Monte Carlo simulation of the gamma-ray source population due to cold gas clouds, assuming a Cold-Dark-Matter-like mass spectrum for the clustering. We find that ~ 280 EGRET sources are predicted by this model, with a median Galactic latitude of 12° for the population, and a median angular size of 2.2° . The latitude and size distributions are consistent with the UID EGRET source data, but the source counts are clearly overpredicted. On the basis of these results we propose that clusters of cold gas clouds comprise the majority population of the observed UID EGRET sources. Our interpretation implies that there should be microwave counterparts to most of the UID sources, and will thus be strongly constrained by data from the present generation of microwave anisotropy experiments.

Subject headings: galaxies: Milky Way — galaxies: halos — dark matter — gamma-rays: general — cosmic-rays: general — ISM: clouds

1. Introduction

The nature of the UnIDentified (UID) EGRET sources (Hartman et al 1999) is one of the most interesting puzzles in contemporary high energy astrophysics. This puzzle persists primarily because of the dimensions — typically of order a degree — of the gamma-ray error boxes: large uncertainties in source position prohibit deep searches for counterparts at other wavelengths. We know, however, that this is only part of the problem: in some cases the EGRET source is bright enough that it can be located quite accurately, yet still no clear counterpart can be found (e.g. Mirabel et al 2000; Reimer et al 2001).

The majority of the discrete sources detected by the EGRET instrument are UID sources (Hartman et al 1999); it is not clear at present whether

they are fundamentally similar to the known GeV emitters, or whether they represent an entirely new population. Because the UID sources are predominantly located at low to mid Galactic latitudes, they must be a Galactic population. This rules out one of the major classes of known discrete celestial GeV gamma-ray sources, namely the flat-spectrum radio quasars as these are extragalactic and hence isotropically distributed on the sky. Much attention has therefore focussed on the possibility that the UID sources are related to massive stars and their evolutionary end-points. In particular there has been intense interest in young pulsars as a contributor to the UID population (e.g. Bailes and Kniffen 1992; Kaaret and Cottam 1996; Roberts, Romani and Johnston 2001; Grenier and Perrot 2001); several of the identified GeV sources are young pulsars (Hartmann et al 1999). How-

ever, the observed latitude distribution of the UID sources is too broad to be readily compatible with young pulsars (Yadigaroglu and Romani 1997). Supernova remnants (Sturner, Dermer and Mattos 1996; Torres et al 2003), molecular clouds and massive star clusters (Montmerle 1979; Benaglia et al 2001) share this difficulty; but Gehrels et al (2001) have noted that the sky distribution of UID sources is consistent with a strong contribution from objects in Gould's Belt, thus supporting a connection with massive stars.

Given the difficulty of detecting counterparts to the UID EGRET population, it is natural to consider the possibility that these sources may be connected with the dark matter problem. The currently popular cosmological model, the Cold Dark Matter model (e.g. Peebles 1993), stipulates that the dark matter is composed of weakly interacting particles; it is possible that these particles are massive – i.e. they are WIMPS – and could yield gamma-rays by annihilation or decay. This possibility has been explored by many authors, e.g. Calcáneo-Roldán and Moore (2000), Bergström, Edsjö and Gunnarsson (2001).

There are of course other types of dark matter. Of particular interest in the present context is baryonic dark matter in the form of cold, dense gas clouds: unlike diffuse gas, cold, dense clouds are difficult to detect directly (Pfenniger, Combes and Martinet 1994; Gerhard and Silk 1996; Combes and Pfenniger 1997; Walker and Wardle 1999). There are many astrophysical motivations for considering dark matter in this form, ranging from the properties of late-type galaxies (Pfenniger, Combes and Martinet 1994; Walker 1999), to observations of radio-wave scintillation (Henriksen and Widrow 1995; Walker and Wardle 1998), and the “Blank Field” SCUBA sources (Lawrence 2001). Indirect constraints – from the small amplitude of fluctuations in the Cosmic Microwave Background (CMB), and from Big Bang Nucleosynthesis – are generally supposed to exclude any significant amount of baryonic dark matter (e.g. Turner and Tyson 1999), but these arguments are not entirely free of loopholes (Hogan 1993; Walker and Wardle 1999) and direct constraints are desirable. There is not yet any direct observational evidence which excludes a substantial fraction of the Galactic dark matter being in the form of cold, dense gas clouds (Pfenniger, Combes and Mar-

tinet 1994; Gerhard and Silk 1996; Walker and Wardle 1999; Rafikov and Draine 2000; Ohishi, Mori and Walker 2003; Walker and Lewis 2003). But the key motivation here for considering this form of dark matter is that gas clouds are expected to emit gamma-rays if they reside in the cosmic-ray disk (e.g. Bloemen 1989), and any unexplained gamma-ray flux might therefore be a signature of dark matter in this form (De Paolis et al 1995; Kalberla, Shchekinov and Dettmar 1999; Sciama 2000). The Galactic gamma-ray halo reported by Dixon et al (1998) has, for example, been interpreted in these terms (De Paolis et al 1999). The low mass ($\sim 10^{-4} M_\odot$) of the individual clouds renders them undetectable by EGRET when they exist in isolation (see §5). However, clustering is ubiquitous in gravitating systems, and we therefore consider the possibility that the UID EGRET sources are simply clusters of cold, dense gas clouds.

The present paper is organised as follows: we begin by describing the model we have employed for the distribution of cold gas clouds (§2), and the emission which is expected from the gas as a result of cosmic-ray interactions (§3); our model cosmic-ray distribution is given in §4; we present the results of our Monte Carlo simulation in §5, and then compare these results to the EGRET data in §6.

2. Dark matter model

To proceed with a calculation we need to specify a model for the clustering and distribution of the dark matter. The success of the modern structure formation paradigm, exemplified by the Cold Dark Matter (CDM) model (e.g. Blumenthal et al 1984; Davis et al 1985; Peebles 1993), argues that any acceptable model must possess clustering properties that are similar to those of CDM, in order to match the data on large-scale-structure. In CDM simulations it is found that the dark matter within individual galaxy halos is clustered into mini-halos, with roughly equal contributions to the total dark matter density being made by all mini-halo mass scales (Kauffmann, White and Guideroni 1993, Moore et al 1999; Klypin et al 1999) — i.e. $dn/dM \propto M^{-2}$, for mini-halos of mass M and number density n . Following Walker, Ohishi and Mori (2003: WOM03

hereafter), we adopt this mass spectrum for our calculations, spanning the mini-halo mass range $0.1 \leq M/M_\odot \leq 10^{10}$. We further assume that all of the Galactic dark matter is in the form of cold gas clouds, clustered into mini-halos. Numerical simulations of structure formation typically show only $\sim 10\%$ of the dark matter within a halo to be clustered into mini-halos (Ghigna et al 1998; Klypin et al 1999). However, these simulations do not have the resolution required to find low mass ($M < 10^8 M_\odot$) mini-halos, and are relevant to only the top 20% (mass fraction) of our adopted spectrum. Assuming that the true clustering spectrum does indeed extend to $M \ll 10^8 M_\odot$, we thus expect that the total mass fraction in mini-halos is actually several times larger than is revealed by simulations. We have therefore adopted the extreme model in which all of the dark matter is clustered; this has the virtue of being a limiting case.

The adopted mini-halo mass spectrum is assumed to be the same throughout the Galaxy, but the normalisation (i.e. total number density of mini-halos) varies in direct proportion to the mean dark matter density of the Galaxy. Gas clouds are a collisional form of dark matter, so that an initially singular isothermal halo develops a core whose radius increases with time (Walker 1999). Simple calculations of this evolution lead to a preferred value for the column density of the individual gas clouds of $\Sigma \simeq 140 \text{ g cm}^{-2}$, and hence a preferred model for the Galactic dark matter density distribution. We adopt this model, namely an isothermal sphere, with circular speed of 220 km s^{-1} , and a core radius of 6.25 kpc (Walker 1999).

The density profile of the individual mini-halos themselves is also of some interest to us, in that it determines the apparent structure of the gamma-ray sources. At present there is little motivation for a detailed appraisal of these properties. The key point, however, is that the mini-halos are not expected to be point-like gamma-ray sources, and we are therefore interested in estimating their sizes. We follow WOM03 in assuming (see Ghigna et al 1998; Moore et al 1999) that the mini-halos are tidally truncated at perigalacticon, with the location of the latter estimated as one half of the Galactocentric radius of the mini-halo. This leads to gamma-ray sources with estimated angular sizes

of order degrees.

3. Gamma-ray emissivity

For high column-density gas clouds, predicting the effects of cosmic-ray bombardment is more complicated than for diffuse gas because the cosmic-ray spectrum is substantially modified by transport through the cloud (Kalberla, Shchekinov and Dettmar 1999; Sciama 2000). Scattering and absorption of the emergent gamma-rays is similarly important. We have therefore used the Monte Carlo event simulator GEANT¹ to estimate the gamma-ray spectrum resulting from cosmic-ray bombardment of dense gas clouds (Ohishi, Mori and Walker 2003). By using GEANT we are able to study the transport of cosmic-rays into dense gas clouds, and their resulting gamma-ray emission, with all relevant interactions included. We employ the results of GEANT simulations for clouds of mean column-density 100 g cm^{-2} , this being the closest, simulated case to our preferred value of Σ (§2). For the most part we shall need only the integrated gamma-ray emissivity of the gas clouds. In the solar neighbourhood we estimate the $> 100 \text{ MeV}$ emissivity due to cosmic-ray hadrons (mainly protons) to be $J_p = 5.1 \times 10^{-2} \text{ ph g}^{-1} \text{s}^{-1}$, while that due to cosmic-ray electrons is $J_e = 5.2 \times 10^{-3} \text{ ph g}^{-1} \text{s}^{-1}$ (Ohishi, Mori and Walker 2003). Here we have adopted the median cosmic-ray proton spectrum of Mori (1997), and the cosmic-ray electron spectrum of Skibo and Ramaty (1993). The total emissivity is thus estimated to be $J = J_p + J_e = 5.6 \times 10^{-2} \text{ ph g}^{-1} \text{s}^{-1}$.

4. Cosmic-rays

Most of our information on the Galactic cosmic-ray spectrum comes from direct observation of energetic particles in the solar neighbourhood, and we know very little about the spectrum at other locations in the Galaxy. Although it is possible to construct theoretical models of the cosmic-ray spectrum and distribution throughout the Galaxy, based on assumed sources, sinks and diffusive particle propagation (e.g. Porter and Protheroe 1997, Strong, Moskalenko and Reimer 2000), such models introduce an additional layer of complexity

¹<http://wwwinfo.cern.ch/asd/geant>

which is unwarranted in the present context. Here we adopt the simple assumption that the shape of the cosmic-ray spectrum is the same throughout the Galaxy.

It then remains to specify the cosmic-ray energy-density as a function of position in the Galaxy. Webber, Lee and Gupta (1992: WLG92) constructed numerical models of cosmic-ray propagation in the Galaxy; they did not give any analytic forms for their model cosmic-ray distributions, but an appropriate analytic approximation can be deduced from the results which they obtained. They found that the cosmic-ray radial distribution reflects, in large part, the radial dependence of cosmic-ray sources, with a modest smoothing effect introduced by diffusion. We have therefore adopted WLG92's preferred model (their model #3) for the radial distribution of sources as our model for the radial distribution of cosmic-rays.

The various spectra of cosmic-ray isotope ratios considered by WLG92 favour models in which the diffusion boundaries are in the range 2 – 4 kpc above and below the plane of the Galaxy. We adopt the midpoint of this range. WLG92 do not give a simple functional form for the vertical variation of cosmic-ray density within this zone, so we have simply assumed an exponential model: $\exp(-|z|/h)$. We know that in WLG92's models the cosmic-ray density is fixed at zero at the diffusion boundaries, and consequently the scale-height of the exponential should be approximately half of the distance to the diffusion boundary, i.e. $h \simeq 1.5$ kpc.

These considerations lead us to the model cosmic-ray density distribution $U(R, z)$:

$$\frac{U}{U_\odot} = \left(\frac{R}{R_0} \right)^{0.6} \exp[(R_o - R)/\varrho - |z|/h], \quad (1)$$

in terms of cylindrical coordinates (R, z) . Here $R_o \simeq 8.5$ kpc is the radius of the Solar circle, while $\varrho = 7$ kpc, and $h = 1.5$ kpc; $U_\odot = U(R_o, 0)$ is the cosmic-ray density in the Solar neighbourhood. This distribution has the character of a disk with a central hole.

5. Results

Using the model described above, we simulated $\sim 2 \times 10^8$ halos with masses $10^2 \leq M/M_\odot \leq 10^{10}$

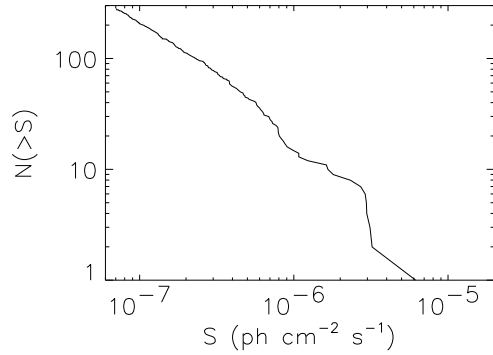


Fig. 1.— The gamma-ray source counts, as a function of flux (above 100 MeV), for the simulated mini-halo population.

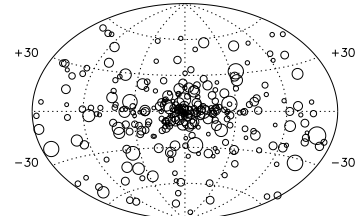


Fig. 2.— Sky distribution of simulated gamma-ray sources lying above the EGRET flux limit (7×10^{-8} ph cm $^{-2}$ s $^{-1}$ above 100 MeV). The size of the circle plotted for each source increases according to the source flux.

located within 50 kpc of the Galactic Centre. The model mini-halo mass spectrum which we utilised extends to lower masses ($0.1 M_{\odot}$); these very-mini-halos (pico-halos?) were not included in the simulation because a negligible fraction of them can be detected (see later). By the same token, the individual gas clouds themselves ($M \sim 10^{-4} M_{\odot}$) are not expected to be detectable by EGRET. In particular, if all of the dark matter is assumed to be in a spherical halo of *unclustered* clouds, then the closest example to the Sun should lie at a distance of order 0.1 pc, and have a flux of order $7 \times 10^{-9} \text{ ph cm}^{-2} \text{ s}^{-1}$ above 100 MeV; this is roughly an order of magnitude below the detection limit of EGRET.

Although the dark halo of the Galaxy extends to very large radii ($\gg 50$ kpc), mini-halos with Galactocentric radii greater than 50 kpc are typically undetectable because of the low cosmic-ray energy density at these radii. The total mass of dark matter simulated is approximately $3.3 \times 10^{11} M_{\odot}$; this is only 8/11 of the total amount of dark matter within the simulated volume, with the remaining 3/11 being made up of clusters in the mass range $10^{-1} \leq M/M_{\odot} < 10^2$.

We find that a fraction $\sim 1.5 \times 10^{-6}$ of the simulated mini-halos have a predicted photon flux above 100 MeV of more than $F = 7 \times 10^{-8} \text{ ph cm}^{-2} \text{ s}^{-1}$, thus placing them above the approximate EGRET threshold (cf. Gehrels et al 2001). In other words, the simulations yield ~ 280 sources bright enough that they should appear in the EGRET catalogue. The source counts, as a function of flux, are shown in figure 1; the relation is clearly flatter than usual Euclidean result ($N \propto S^{-3/2}$), and at low flux levels is well approximated by $N \propto S^{-1}$.

The locations of the synthetic sources on the sky are shown in figure 2, where it can be seen that although they populate the entire sky, they are more concentrated towards the disk of the Galaxy, and are preferentially found toward the central regions. These features are primarily a reflection of our adopted model of the distribution of cosmic-rays in the Galaxy (§4). The median Galactic latitude of the sources is 12° . Dividing the population into two equally-sized groups of low and high latitude sources yields no significant difference in median flux between the two groups.

The mass distribution of the detectable mini-

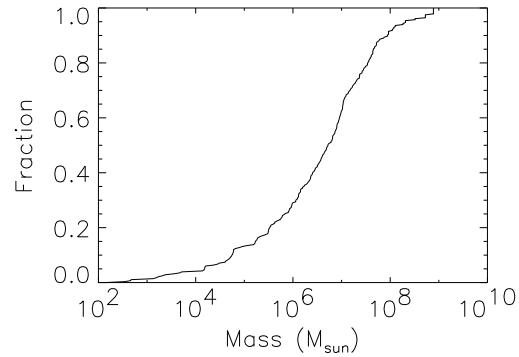


Fig. 3.— The distribution of mini-halo mass, for the synthetic population of sources which lie above the EGRET flux limit. The median value is $5 \times 10^6 M_{\odot}$.

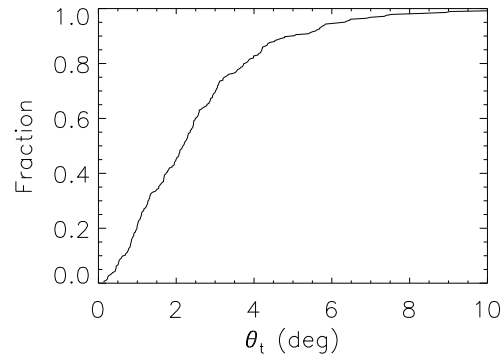


Fig. 4.— The distribution of source radii (tidal radii), for the synthetic population of sources which lie above the EGRET flux limit. The median value is 2.2 degrees.

halos is shown in figure 3. At the high mass end the sources may be very luminous and can thus be detected to large distances, whereas only the closest of the low mass mini-halos are detectable. The competition between increasing mini-halo number density and declining luminosity, towards lower mini-halo masses, results in a characteristic (median) mass of $5 \times 10^6 M_\odot$ for the detectable sources. In the vicinity of the Sun, a mini-halo of this mass is expected to have a luminosity of approximately $8 \times 10^{34} \text{ erg s}^{-1}$, in photons of energy above 100 MeV. This result is in accord with the analysis of the UID EGRET source population by Kambach et al (1996), who concluded that their typical luminosity is $\sim 10^{35} \text{ erg s}^{-1}$. The median line-of-sight distance for the mini-halos with flux greater than the EGRET detection limit is 3.9 kpc.

Bearing in mind that both Active Galactic Nuclei (AGN) and pulsars are effectively point-like gamma-ray sources, the non-trivial angular size predicted for the gamma-ray emission from dark mini-halos is an important feature of the model. We characterise the size of the sources by θ_t , the tidal radius of the mini-halo; this is the radius which encloses all of the flux from the model source. We compute θ_t using the same procedure as WOM03. For a singular isothermal sphere, the surface brightness is $I \propto 1/\theta$ at all radii, and we expect roughly half of the flux to be contained within $\theta_t/2$. The median value of the tidal radius is $\langle \theta_t \rangle = 2.2^\circ$, for sources detectable by EGRET. The full distribution of θ_t is shown in figure 4.

Intrinsic source confusion, i.e. the regime where sources are so numerous that they overlap on the sky, becomes a minor problem in the region around the Galactic Centre. Within 10° latitude/longitude of the Galactic Centre (an area of roughly 400 deg^2), we find 32 sources, covering about 100 deg^2 (the sources are smaller than average). This figure is an overestimate in the sense that our model predicts too many sources — see §6. With more sensitive instrumentation, having a lower flux limit, intrinsic source confusion becomes a major issue, as the mini-halo population covers the entire sky (WOM03).

6. Comparison with observations

It is clear that the model we have presented predicts too many EGRET sources. The entire

EGRET source list contains only about as many sources as our simulation predicts, and many ($\sim 40\%$) of the catalogued sources are considered to be identified. Furthermore, we must expect that there will be many examples of known types of gamma-ray sources, such as pulsars, amongst the UID EGRET sources, implying that our model over-predicts the source count by a factor $\gtrsim 2$. However, it must be acknowledged that the model we have presented involves substantial extrapolation into poorly charted territory and is therefore illustrative, not definitive. There are, for example, considerable uncertainties in the cosmic-ray distribution model, in the shape of the Galaxy's dark halo, and in the mass spectrum of the clustering. In addition, we can immediately point to one aspect of the dark matter model which leads to an over-prediction of the source counts: we have assumed that *all* of the dark matter in the Galactic halo is bound into mini-halos (§2; WOM03), but this cannot be the case. Even if all the dark matter were initially in mini-halos, the process of tidal stripping will gradually unbind material, leading to a significant fraction in the form of dark matter "streams". Considering these uncertainties, we recognise that the over-prediction of source counts is not a fundamental deficiency of the model.

Other basic features of the UID source population can be used to gauge the success of the model: the distribution on the sky; spectra; variability; angular structure; and observations made in other wave-bands. We now address each of these aspects in turn.

6.1. Sky distribution

The model correctly predicts a preponderance of sources at low- to mid-Galactic latitudes, with about the right median latitude (12°) for the population. However, it does not exhibit the two component (thin-disk plus thick-disk) source population which the data suggest (Gehrels et al 2001).

Figure 2 shows a relatively strong concentration towards the Galactic Centre region, compared to the data. However, in this region the predicted source density is sufficiently high that source confusion is expected to be a major problem with EGRET observations of a such a population. The predicted confusion is predominantly instrumental, because the sources are typically unresolved (see §6.4). We find approxi-

mately 100 sources within $\pm 30^\circ$ of latitude and longitude of the Galactic Centre – an area of roughly 3400 deg². By comparison the point-spread-function of EGRET has a Full-Width Half-Maximum (FWHM) of approximately 4° (see §6.4), implying that this entire region appears, to EGRET, to be “covered” with overlapping sources.

6.2. Spectra

The spectrum predicted by the present model is given in Ohishi, Mori and Walker (2003): it exhibits a peak power – i.e. a peak in $E^2 dN/dE$ – at several-hundred MeV. At this point the spectrum rolls over from $dN/dE \propto E^{-1}$, at low energies, approaching $E^{-2.75}$ at $E \gg 1$ GeV.

In comparing this prediction with the data (e.g. Merck et al 1996), there are two important points to bear in mind. First, the model gamma-ray emission spectrum is unique only by default: we don’t know the cosmic-ray spectrum elsewhere in the Galaxy. The simple fact that various gamma-ray spectra are observed should therefore not be used as an argument against the present model. We note that the diffuse Galactic plane emission at $E \gtrsim 1$ GeV (Hunter et al 1997) is difficult to understand if the Galactic cosmic-ray spectrum is everywhere the same as in the solar neighbourhood, suggesting that the typical cosmic-ray spectrum may be harder than measured locally (Mori 1997).

Secondly, the sources are predicted to be extended, with low-intensity wings on the profile extending out to $\sim 2^\circ$, typically. Although the spectrum should be uniform across the source, the fact that the point-spread function of the detector changes with energy, coupled with the low-level “wings” on the source profile, could lead to spurious estimates of spectral shapes. In particular, some fraction of the source flux will be absorbed into the estimate of the background intensity, and this fraction will vary with photon energy. These problems, coupled with the low signal-to-noise ratio of many of the UID sources, make it difficult to assess the success of the model spectral predictions.

6.3. Variability

The model we have presented involves emission which is intrinsically steady on observationally accessible time-scales; it is therefore not relevant to any sources which are known to vary significantly. Most of the UID EGRET sources are not bright enough to permit strong constraints on their variability. There is no consensus in the literature regarding the variability of the UID sources: McLaughlin et al (1996) find that only a small fraction, roughly one in six, of the UID EGRET sources are significantly variable (see also Wallace et al 2000); by contrast Torres et al (2001) suggest that the fraction may be as large as one third, in the case of low-latitude UID sources (see also Torres, Pessah and Romero, 2001, and Tompkins 1999). We note that large-amplitude variations do not sit easily with the multiple/extended source designation carried by $\sim 50\%$ of the UID EGRET sources (Hartman et al 1999).

6.4. Angular Structure

Although the estimated angular sizes of the detectable mini-halos are large (of order degrees), the resolving power of EGRET is quite modest, with a point-spread-function of 5° Full-Width-Half-Maximum (FWHM) at 100 MeV (Thompson et al 1993). (The in-flight calibration data are consistent with the pre-launch calibration in respect of the point-spread-function — Esposito et al 1999.) The EGRET angular resolution improves with increasing energy, scaling roughly as $E^{-0.534}$. However, if dN/dE is close to E^{-2} , half of the photons contributing to a source detection are within a factor ~ 2 of the low-energy threshold. We therefore adopt a FWHM of 4° as the relevant instrumental width; sources would thus need to be at least 8° across in order to be fully resolved. For an isothermal density distribution within each mini-halo (§5), half of the total flux is contained within a diameter approximately equal to θ_t . Referring to figure 4 we then find that only a tiny fraction of the synthetic population could be fully resolved by EGRET.

If the instrumental FWHM is comparable to the source size then the source structure will not be resolved, but the data can nevertheless indicate that the source is extended, by virtue of the observed intensity profile being broader than

the point spread function. Most of the synthetic sources fall into this category. It is notable that half of the UID EGRET sources are recorded as extended/multiple by Hartman et al (1999). (The two possibilities cannot be differentiated if the source structure is not fully resolved.)

6.5. Counterparts at other wavelengths

The basic criterion for an EGRET source to be classified as “UID” is that it should not have an obvious counterpart at other wavelengths. The population we have modelled clearly meets this requirement because the emission comes from “dark” matter. The detectability of cold, dense gas has been discussed by a number of authors: Pfenniger, Combes and Martinet (1993); Gerhard and Silk (1996); Combes and Pfenniger (1997); Walker and Wardle (1999); and Sciama (2000). Perhaps the simplest and most robust of expectations is that there will be thermal emission from the clouds, implying bright microwave sources co-incident with the gamma-ray sources. An important point to note is that gamma-ray and microwave luminosities are both proportional to mini-halo mass and cosmic-ray density; consequently the microwave flux can be estimated simply by scaling the observed EGRET flux (Wardle and Walker 1999; Sciama 2000).

To determine the bolometric microwave flux we need only take the ratio of the thermal emissivity due to cosmic-rays ($\Gamma_0 \simeq 10^{-4} \text{ erg s}^{-1} \text{ g}^{-1}$; WOM03), to the gamma-ray emissivity ($J = J_p + J_e \simeq 5.6 \times 10^{-2} \text{ ph s}^{-1} \text{ g}^{-1}$ above 100 MeV; §3), yielding a microwave flux of $S \simeq 1.8 \times 10^{-10} F_7 \text{ erg cm}^{-2} \text{ s}^{-1}$. Here the gamma-ray flux above 100 MeV is $10^{-7} F_7 \text{ ph cm}^{-2} \text{ s}^{-1}$. The atmospheric temperature is estimated to be in the range $4.2 - 4.9 \text{ K}$, if the individual clouds have mass $M \sim 10^{-4} - 10^{-5} M_\odot$ (WOM03). The principal remaining uncertainty then lies with the nature of the emitted spectrum: we have previously suggested a blackbody spectrum (WOM03), whereas Lawrence (2001) concludes that this is inconsistent with the observed spectrum of the Blank Field SCUBA sources (which objects he interprets in terms of cold, planetary-mass gas clouds). More generally we can take $S_\nu \propto \nu^\alpha B_\nu$, with $\alpha = 0$ for blackbody emission, and $\alpha = 2$ for emission from small particles whose absorption increases in proportion to ν . Lawrence (2001) concludes that

the latter spectrum is consistent with the data on the Blank Field SCUBA sources, providing $4.7 < T(\text{K}) < 6.4$. Here we restrict attention to two cases which adequately represent the plausible range of thermal emission spectra for the dense gas: a $T = 4.2 \text{ K}$ blackbody, and a $T = 4.9 \text{ K}$ “dusty” ($\alpha = 2$) spectrum.

Our adopted spectra differ greatly in the expected flux at radio frequencies, where we are far below the peak thermal emission — see figure 5. At low frequencies the two spectral models can be approximated by $S_\nu \simeq 4.2 \nu^2 F_7 \text{ mJy}$ (blackbody) and $S_\nu \simeq 1.4 \times 10^{-5} \nu^4 F_7 \text{ mJy}$ (dust), with ν in GHz. However, even in the blackbody case, where the radio emission is relatively strong, the predicted flux would be difficult to detect because it is so extended. Taking the bright UID EGRET source 3EG J1835+5918 as an example (Hartman et al 1999; Mirabel et al 2000; Reimer et al 2001), with $F_7 \simeq 7$, we find a predicted flux at 1.4 GHz of roughly 60 mJy in the blackbody case. This estimate is well above the point source detection limit of the observations, reported by Mirabel et al (2000), of 2.5 mJy. However, a mini-halo is certainly not point-like. In fact it would fill the primary beam of the radio telescope, and would be resolved-out on all but the shortest interferometric baselines. The very extended sources predicted by the present model are expected to be difficult to detect using radio interferometers configured for high resolution imaging.

7. Discussion

Although the predicted microwave counterparts to UID EGRET sources are not expected to have been detected in the counterpart searches to date, they could be revealed in the near future by some of the various experiments designed to study anisotropies in the Cosmic Microwave Background (CMB). In particular, the MAP satellite², has now completed a sensitive all-sky survey, at several frequencies, and the data are about to be released. Should MAP have detected the predicted microwave counterparts? The answer to this question depends on the spectrum of the emission, because all of the MAP frequencies are well below the thermal peak. Even considering the highest frequency channel (90 GHz), the two spectral mod-

²<http://map.gsfc.nasa.gov>

els differ by a large factor in their predicted flux. If the emission is blackbody, then $S_\nu \simeq 20 F_7$ Jy, but only $S_\nu \simeq 0.6 F_7$ Jy for the “dust” model (see figure 5). The point-source (i.e. single pixel) detection limit for MAP at this frequency should be approximately 1.7 Jy (5σ , and we have taken the CMB contribution to be roughly equal to the thermal noise of the instrument). On this basis we do not expect the typical UID sources to be detected by MAP if they have a “dusty” spectrum.

Even if the mini-halos have a blackbody spectrum they might not be detected by MAP, because its 0.3° pixels are substantially smaller than the predicted mini-halo sizes. For an isothermal mini-halo density profile, the enclosed flux varies roughly in proportion to radius. With a predicted median source radius of 2.2° , it is evident that the largest single-pixel flux expected from a typical mini-halo is not much above the MAP detection limit. Computing the peak single-pixel flux for each source in our simulation, we expect that only 40% of the predicted population ought to be detectable by MAP even if the spectra are blackbody. However, we note that sources which are individually undetected may still be useful for constraining the typical microwave/gamma-ray flux ratio of the UID EGRET population.

Other satellite and balloon-borne CMB experiments will provide robust constraints on the model we have presented, by virtue of observing close to the predicted thermal peak of the mini-halos. In particular, the High Frequency Instrument on the Planck satellite³ and its prototype, the balloon-borne Archeops (Benoit et al 2002), will map the sky at 353 and 545 GHz, sandwiching the point – around 400 GHz (see figure 5) – where our model spectra cross. At these frequencies the predicted flux of a typical UID EGRET source ($F_7 = 1$) is of order 30 Jy, for either spectral model. By contrast, the limiting flux (5σ) for Planck, at 353 GHz, will be 100 mJy in a single (5 arcmin) pixel, and roughly 5 Jy for a source of 2.2° radius. (Observing at these high frequencies has the additional advantage of less confusion from the degree-scale CMB anisotropies.) Planck should therefore detect microwave counterparts to any of the UID EGRET sources in which the gamma-rays arise from cosmic-ray interactions with dense gas. We

note that a substantial fraction of the sky has already been mapped by the Archeops experiment (Benoit et al 2002), and UID EGRET source counterparts might be present in the existing data. Counterparts are best searched for, initially, well away from the Galactic plane as the latter region is likely to be confused at high frequencies. Scaling from the Planck sensitivity estimates, using the estimated duration and coverage – 2 year mission with full sky coverage, for Planck, versus 24 hour Archeops dataset covering 25% of the sky – we estimate that the flux limit of Archeops, for the extended microwave sources we predict, should be approximately 70 Jy. Hence UID EGRET sources brighter than $3 \times 10^{-7} \text{ ph cm}^{-2} \text{s}^{-1}$ ($> 100 \text{ MeV}$) may have counterpart microwave sources found in the Archeops data.

We note that the balloon-borne MAXIMA and BOOMERANG experiments also covered frequencies close to the thermal peak of cold gas emission, but these experiments covered only $\sim 1\%$ of the sky (Hanany et al 2000; Coble et al 2003), and these data are therefore of limited utility in the present context. Ground-based studies are similarly limited to small patches of the sky, when observing at 400 GHz, but would nevertheless be helpful if the UID EGRET source population is specifically targetted for observations.

If microwave counterparts are discovered, then we will be able to study the density profiles of dark matter mini-halos directly. Further to the properties noted in §2 for the individual source profiles, we can make some generic predictions for their structure: (i) the intensity should rise to a high central peak, but there should be a core (Walker 1999) in the surface-brightness profile; (ii) the limb of the source should exhibit a sharp cut-off due to tidal truncation; and (iii) there may be tidal streams extending along the mini-halo’s orbit.

In addition to tidal streams associated with identifiable mini-halos, it is expected that some mini-halos have been completely disrupted by the tidal fields they have experienced. In these cases the tidal streams are not associated with a bound cluster, and thus represent a distinct category of microwave/gamma-ray source predicted by the model. Shells with sharply-defined edges could also appear in the microwave/gamma-ray maps, as these are a common feature of tidal debris (Hernquist and Quinn 1988; Hernquist and Spergel

³<http://sci.esa.int/home/planck>

1992).

The Gamma-ray Large Area Space Telescope⁴ (GLAST) will provide a significant advance in our understanding of the UID sources, because GLAST will be much more sensitive than EGRET and will have better angular resolution. These improved capabilities will permit powerful tests of the model we have presented. However, the data from MAP and the balloon-borne CMB experiments will be available on a much shorter time-scale than those from GLAST, and it should be possible to make considerable progress with the microwave data alone. In particular, our prediction of bright, extended, thermal microwave counterparts is unique amongst existing models of the UID EGRET population.

Finally we note that some of the UID EGRET sources are sufficiently bright that they may be detectable by ground-based TeV telescopes (Aharonian et al 1997), even if their spectra are as steep as $E^{-2.75}$ between the GeV and TeV bands. Studying UID sources at TeV energies may permit their nature to be discerned. For example, the extended nature of the sources predicted by the present model is unusual for gamma-ray sources, and the slightly extended (6 arcminute) TeV source, in the vicinity of 3EG J2033+4118, reported by Aharonian et al (2002) is of interest in this context.

8. Conclusions

If our Galaxy contains a significant component of dark matter in the form of cold, dense gas clouds, clustered into large aggregates, some of those clusters should have been detected by EGRET. Using a CDM-like mass spectrum for the clustering, we have shown that the predicted gamma-ray source population has properties which are broadly similar to those of a large fraction of the UID EGRET sources. In particular: the Galactic latitude distribution and the source size distribution anticipated in the model find support in the EGRET data. Furthermore the intrinsically “dark” nature of the predicted sources naturally explains most of the difficulty in finding counterparts; however, the large angular size of the clusters also plays a role, because

counterpart searches to date have had poor sensitivity to \sim degree-sized sources. The total number of UID sources predicted by the model is too large, particularly bearing in mind that many of the observed UID sources are likely to be examples of known types of gamma-ray emitters. Data returned by the various CMB experiments will provide a powerful test of the interpretation we have presented: counterpart thermal microwaves should be detected from the cold gas, and the source structure should be resolved.

MAW thanks Gordon Garmire and Eric Feigelson for emphasising the importance of the gamma-ray data, and for helpful discussions on the relevant physics. We thank Ben Moore for advice on modelling the mini-halo population, and Simon Johnston for helpful comments on the manuscript. The Referee’s comments also improved the paper.

REFERENCES

Aharonian F.A., Hofmann W., Konopelko A.K., Völk H.J. 1997 APh 6, 369

Aharonian F.A. et al 2002 A&A 393, L37

Bailes M., Kniffen D.A. 1992 ApJ 391, 659

Benaglia P., Romero G.E., Stevens I.R., Torres D.F. 2001 A&A 366, 605

Benoît A. et al 2002 APh 17, 101

Bergström L., Edsjö J., Gunnarsson C. 2001 PhRvD 63(8), 3515

Bloemen H. 1989 ARAA 27, 469

Blumenthal G., Faber S.M., Primack J.R., Rees M.J. 1984 Nature 311, 527

Calcáneo-Roldán C., Moore B. 2000 PhRvD 62(12), 3005

Combes F., Pfenniger D. 1997 A&A 327, 453

Coble K. et al 2003 ApJS (Submitted) (astro-ph/0301599)

Davis M., Efstathiou G., Frenk C.S., White S.D.M. 1985 ApJ 292, 371

De Paolis F., Ingrosso G., Jetzer Ph., Roncadelli M. 1995 A&A, 295, 567

De Paolis F., Ingrosso G., Jetzer Ph., Roncadelli M. 1999 ApJL, 510, L103

⁴<http://glast.gsfc.nasa.gov>

Dixon D.D., Hartmann D.H., Kolaczyk E.D., Samimi J., Diehl R., Kanbach G., Mayer-Hasselwander H., Strong A.W. 1998 *NewAst* 3, 539

Esposito J.A. et al 1999 *ApJS* 123, 303

Gehrels N., Macomb D.J., Bertsch D.L., Thompson D.J., Hartman R.C. 2001 *Nature*, 404, 363

Gerhard O., Silk J. 1996, *ApJ*, 472, 34

Ghigna S., Moore B., Governato F., Lake G., Quinn T., Stadel J. 1998 *MNRAS* 300, 146

Gregory P.C., Vavasour J.D., Scott W.K., Condon J.J. 1994 *ApJS* 90, 173

Grenier I.A., Perrot C.A. 2001 *AIP Conf. Proc.* 587, 649

Hanany S. et al 2000 *ApJL* 545, L5

Hartman R.C. et al 1999 *ApJS* 123, 79

Henriksen R.N., Widrow L.M. 1995, *ApJ*, 441, 70

Hernquist L., Quinn P.J. 1988 *ApJ* 331, 682

Hernquist L., Spergel D.N. 1992 *ApJL* 399, L117

Hogan C.J. 1993 *ApJL* 415, L63

Hunter S.D. et al 1997 *ApJ* 481, 205

Kaaret P., Cottam J. 1996 *ApJL* 462, L35

Kalberla P.M.W., Shchekinov Yu.A., Dettmar R.-J. 1999 *A&A* 350, L9

Kanbach G. et al 1996 *A&AS* 120, 461

Kauffmann G., White S.D.M., Guideroni B. 1993 *MNRAS* 264, 201

Klypin A., Kravtsov A.V., Valenzuela O., Prada F. 1999 *ApJ* 522, 82

Lawrence A. 2001 *MNRAS* 323, 147

McLaughlin M.A., Mattox J.R., Cordes J.M., Thompson D.J. 1996 *ApJ* 473, 763

Merck M. et al 1996 *A&AS* 120, 465

Mirabel N., Halpern J.P., Eracleous M., Becker R.H. 2000 *ApJ* 541, 180

Montmerle T. 1979 *ApJ* 231, 95

Moore B., Ghigna S., Governato F., Lake G., Quinn T., Stadel J., Tozzi P. 1999 *ApJL* 524, L19

Mori M. 1997 *ApJ* 478, 225

Ohishi M., Mori M., Walker M.A. 2003 (In preparation)

Peebles P.J.E. 1993 "Principles of Physical Cosmology" (PUP, Princeton)

Pfenniger D., Combes F., Martinet L. 1994, *A&A*, 285, 79

Porter T.A., Protheroe R.J. 1997 *Nucl. Part. Phys.* 23, 1765

Rafikov R.R., Draine B.T. 2001 *ApJ* 547, 207

Reimer O., Brazier K.T.S., Carramiñana A., Kanbach G., Nolan P.L., Thompson D.J. 2001 *MNRAS* 324, 772

Roberts M.S.E., Romani R.W., Johnston S. 2001 *ApJL* 561, L187

Sciama D.W. 2000 *MNRAS* 312, 33

Skibo J.G., Ramaty R. 1993 *A&AS* 97, 145

Strong A.W., Moskalenko I.V., Reimer O. 2000 *ApJ* 537, 763

Sturner S.J., Dermer C.D., Mattox J.R. 1996 *A&AS* 120, 445

Thompson D.J. et al 1993 *ApJS* 86, 629

Tompkins W.F. 1999 PhD Thesis (Stanford University) (astro-ph/0202141)

Torres D.F., Pessah M.E., Romero G.E. 2001 *Ast. Nachr.* 322, 223

Torres D.F., Romero G.E., Combi J.A., Benaglia P., Andernach H., Punsly B. 2001 *A&A* 370, 468

Torres D.F., Romero G.E., Dame T.M., Combi J.A., Butt Y.M. 2003 *PhRep*, Submitted (astro-ph/0209565)

Turner M.S., Tyson J.A. 1999 *RModPhys* 71, S145

Walker M.A. 1999 *MNRAS* 308, 551

Walker M.A., Lewis G.F. 2003 *ApJ*, Submitted (astro-ph/0212345)

Walker M.A., Ohishi M., Mori M. 2003 *ApJ*, Submitted (astro-ph/0210483) (WOM03)

Walker M., Wardle M. 1998 *ApJ* 498, L125

Walker M., Wardle M. 1999 *PASA* 16, 262

Wallace P.M., Griffis N.J., Bertsch D.L., Hartman R.C., Thompson D.J., Kniffen D.A., Bloom S.D. 2000 *ApJ* 540, 184

Wardle M., Walker M. 1999 *ApJL* 527, L109

Webber W., Lee M., Gupta M. 1992 *ApJ* 390, 96 (WLG92)

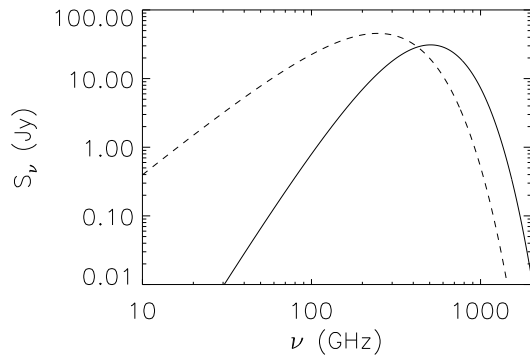


Fig. 5.— Model mini-halo thermal spectra. The dashed line shows a blackbody spectrum at $T = 4.2$ K, and the solid line shows a “dusty” ($\alpha = 2$) spectrum at $T = 4.9$ K. The thermal flux (S_ν) scales in direct proportion to the gamma-ray flux, and this plot is made for a gamma-ray flux of 10^{-7} ph cm $^{-2}$ s $^{-1}$ above 100 MeV.